Experimental determination of the core-excited electron density of states

2006 J. Phys.: Condens. Matter 18 7327

(http://iopscience.iop.org/0953-8984/18/31/025)

INSTITUTE OF PHYSICS PUBLISHING JOURNAL OF PHYSICS: CONDENSED MATTER

J. Phys.: Condens. Matter **18** (2006) 7327–7336 doi:10.1088/0953-8984/18/31/025

Experimental determination of the core-excited electron density of states

J A Soininen[1], A Mattila[1], J J Rehr[2], S Galambosi[1] and K Hämäläinen[1]

[1] Division of X-ray Physics, Department of Physical Sciences, University of Helsinki, POB 64, FI-00014, Finland
[2] Department of Physics, University of Washington, Seattle, WA 98195-1560, USA

Received 11 April 2006, in final form 21 June 2006
Published 21 July 2006
Online at stacks.iop.org/JPhysCM/18/7327

Abstract

We present an implementation of a method to determine different components of the local density of states in the presence of a core hole from inelastic x-ray scattering experiments. The only theoretical input needed beyond experimental data are the embedded atom transition matrix elements. In this work these matrix elements are calculated using a real-space multiple scattering approach. We apply the method to x-ray Raman scattering data for the boron K-edge in MgB_2. The capability of the approach is demonstrated by separating the density of π-, σ- and s-type states at the boron site in MgB_2.

(Some figures in this article are in colour only in the electronic version)

1. Introduction

Core-level spectroscopies are often used to obtain components of the density of empty states under the influence of a core hole. The motivation is that from the core-hole perturbed density of states (DOS), one can also learn about the empty electron states of the system in its ground state. From the DOS one can draw conclusions regarding the chemical environment (i.e. bond numbers, orientation, nearest neighbour distances, oxidation states, etc) of the core-excited site. In core-excited spectroscopies the quantity directly obtained from experiment is the unoccupied, angular-momentum projected local density of states (LDOS) at a given site, weighted by the transition matrix elements. For example, in x-ray absorption spectroscopy (XAS), the matrix elements are calculated using dipole or quadrupole operators (see for example [1]). In the case of non-resonant x-ray Raman scattering, momentum transfer-dependent matrix elements are used instead [2, 3]. When using synchrotrons as a source in XAS experiments, it is possible to control the polarization state of the incident photons. By changing the direction of the linear polarization of the x-rays with respect to sample orientation, one can obtain information on the anisotropy of the empty electron states in the target material. Essentially the same information can be obtained with x-ray Raman scattering by varying the direction of the momentum transfer [4, 5] with respect to sample orientation. However, in

inelastic x-ray scattering one can also change the magnitude of the momentum transfer, thus changing the weights of the different components of the LDOS in the measured spectra [6, 7]. At low momentum transfers (i.e., the dipole limit), standard analysis tools developed for XAS can be used, and the momentum transfer dependence of XRS is seldom exploited. However, recent studies [8–12] have shown that, with modern theoretical tools, it is possible to use the momentum transfer dependence to obtain more detailed information about the sample.

The analysis of core-excited state spectroscopies is usually complicated for a number of reasons. Although the excitation operator involved is a single-particle operator, the energy spectrum itself is a result of intricate many-particle processes and final state effects [6, 13]. In principle, the entire system responds to the creation of a core hole. In order to analyse the spectra, the final state density of states has to be calculated including additional many-particle processes such as inelastic losses [1]. The many-particle nature of the excitation process is the main reason why the experimental spectra are often difficult to interpret and predict. However, with current computational methods the atomic-like single-particle excitation matrix elements can be calculated to good accuracy. If one uses such an approximation for this essentially single-particle property to determine a complicated many-body function, it will then allow a quantitative analysis and comparison with various experimental methods.

In this work we have implemented a recently proposed scheme [14] to use the XRS matrix elements calculated with a real-space multiple scattering method to determine the local density of states from XRS experiments. We have carefully tested the numerical stability of the approach and analysed the limitations of current approximations to the exchange correlation potential. Finally, we have applied the method to recent experimental XRS results for the boron K-edge in MgB_2 [12] to resolve the s- and p-types of local densities of states for the boron site.

2. Scheme

In the non-relativistic Born approximation the double differential cross-section for x-ray Raman scattering can be written as [2, 3]

$$\frac{\mathrm{d}^2\sigma}{\mathrm{d}\Omega\,\mathrm{d}\omega} = \left(\frac{\mathrm{d}\sigma}{\mathrm{d}\Omega}\right)_{\mathrm{Th}} S(\mathbf{q},\omega). \tag{1}$$

Here the Thomson cross-section $(\mathrm{d}\sigma/\mathrm{d}\Omega)_{\mathrm{Th}}$ can be expressed in terms of the incoming (scattered) photon polarization vector and energy $\{\hat{\boldsymbol{\varepsilon}}_1, \omega_1\}$ ($\{\hat{\boldsymbol{\varepsilon}}_2, \omega_2\}$) as

$$\left(\frac{\mathrm{d}\sigma}{\mathrm{d}\Omega}\right)_{\mathrm{Th}} = r_0^2(\hat{\boldsymbol{\varepsilon}}_1 \cdot \hat{\boldsymbol{\varepsilon}}_2)^2 \frac{\omega_2}{\omega_1},$$

where r_0 is the classical electron radius. We assume here that the energy regime is such that the resonant term in the Kramers–Heisenberg equation [2] can be neglected. In the scattering process momentum $\mathbf{q}$ and energy ω are transferred to the target. The sample-dependent part of the cross-section is given by the dynamic structure factor $S(\mathbf{q},\omega)$. When ω is close to the core electron binding energy, $S(\mathbf{q},\omega)$ for the core state $|i\rangle$ can be expressed using Fermi's golden rule:

$$S_{\mathrm{i}}(\mathbf{q},\omega) = \sum_{\mathrm{f}} |\langle f|\mathrm{e}^{\mathrm{i}\mathbf{q}\cdot\mathbf{r}}|i\rangle|^2 \delta(\hbar\omega + E_{\mathrm{i}} - E_{\mathrm{f}}), \tag{2}$$

where E_{i} (E_{f}) is the initial (final) state quasiparticle energy of the electron. Within the real-space multiple scattering formalism we can express $S_{\mathrm{i}}(\mathbf{q},\omega)$ with the help of the final state

multiple scattering matrix (MSM) $\rho_{L,L'}(E) = (-1/\pi)\,\mathrm{Im}\,G_{L,L'}(E)$ [14][3] as

$$S_\mathrm{i}(\mathbf{q},\omega) = \sum_{LL'} M_L(-\mathbf{q},E)\rho_{L,L'}(E)M_{L'}(\mathbf{q},E). \tag{3}$$

Here $G_{LL}(E)$ is the final state electron Green's function for the core-excited site, $E = \omega + E_\mathrm{i}$, and L denotes the angular momentum channel $L = (l,m)$. For the remainder of this paper we will concentrate on excitations from a given core level $|i\rangle$ and suppress the index i from $S_\mathrm{i}(\mathbf{q},\omega)$ for clarity. The matrix elements $M_L(\mathbf{q},E)$ are expressed using the scattering state $R_L(E)$ for the embedded atom and the core-state $|i\rangle$ as

$$M_L(\mathbf{q},E) = \langle R_L(E)|\mathrm{e}^{\mathrm{i}\mathbf{q}\cdot\mathbf{r}}|i\rangle.$$

A similar expression was given by Doniach *et al* [6], although they used a simpler approximation for the wavefunctions in the matrix element. It is important to realize that all the complicated many-particle physics are in the MSM $\rho_{L,L'}(E)$, while the transition matrix elements $M_L(\mathbf{q})$ are essentially properties of an embedded atom.

In principle, the use of the momentum transfer direction and magnitude in the calculated matrix elements, combined with equation (3), could be used to determine the complete matrix $\rho_{L,L'}(E)$. However, due to symmetry properties of the system, the MSM is often a diagonal matrix $\rho_{L,L'}(E) = \delta_{LL'}\rho_L(E)$, or can be assumed to be so to a good approximation. Then the dynamic structure factor becomes

$$S(\mathbf{q},\omega) = \sum_L |M_L(\mathbf{q},E)|^2\rho_L(E). \tag{4}$$

When the plane wave transition operator in the matrix element is expanded using spherical harmonics Y_{lm} and Bessel functions j_l,

$$\exp(\mathrm{i}\mathbf{q}\cdot\mathbf{r}) = 4\pi\sum_{lm} i^l j_l(qr)Y^*_{lm}(\hat{\mathbf{q}})Y_{lm}(\hat{\mathbf{r}}), \tag{5}$$

it becomes clear that the spectral weights of different excitation channels (denoted by L) will change as the magnitude q is varied. This $\mathbf{q}$-dependence is analysed in detail in [14], and earlier in [6, 15]. For polycrystalline samples equation (4) is further simplified due to averaging over the direction of $\mathbf{q}$, and yields

$$S(q,\omega) = \sum_l (2l+1)|M_l(q,E)|^2\rho_l(E). \tag{6}$$

The matrix elements in this case can be written with the help of 3-j symbols and the radial part $R_\mathrm{i}(r)$ of the core state wavefunction as [15]

$$|M_l(q,E)|^2 = (2l_\mathrm{i}+1)\sum_{l'}(2l'+1)\left|\begin{pmatrix} l_\mathrm{i} & l' & l \\ 0 & 0 & 0\end{pmatrix}\int r^2\,\mathrm{d}r\; R_l(r,E)\,j_{l'}(qr)R_\mathrm{i}(r)\right|^2. \tag{7}$$

The method proposed in [14] is simply to use the calculated matrix elements $M_L(\mathbf{q},E)$ (or $M_l(q,E)$) and to treat equations (4) and (6) as linear relations between the matrix $\rho_L(E)$ (or $\rho_l(E)$) and the dynamic structure factor. This will enable us to determine $\rho_L(E)$ (or $\rho_l(E)$) from experiments with different momentum transfers $\{\mathbf{q}_\mathrm{i}\}$ by solving the linear equations

$$\begin{pmatrix} S(q_1,\omega) \\ S(q_2,\omega) \\ \vdots \\ S(q_N,\omega)\end{pmatrix} = \begin{pmatrix} |M_0(q_1,E)|^2 & |M_1(q_1,E)|^2 & \cdots & |M_l(q_1,E)|^2 \\ |M_0(q_2,E)|^2 & |M_1(q_2,E)|^2 & \cdots & |M_l(q_2,E)|^2 \\ \vdots & \vdots & \ddots & \vdots \\ |M_0(q_N,E)|^2 & |M_1(q_N,E)|^2 & \cdots & |M_l(q_N,E)|^2\end{pmatrix}\begin{pmatrix}\rho_0(E) \\ \rho_1(E) \\ \vdots \\ \rho_l(E)\end{pmatrix}, \tag{8}$$

in the least squares sense. In practice we have also found that it is often sufficient at low momentum transfer to assume that only dipole-allowed transitions contribute to the

[3] Without loss of generality we have assumed here that $\mathbf{q}$ is along the Cartesian z-axis.

spectrum. Then we can determine the p-type LDOS as $\rho_1(E) = S(q_1, \omega)/|M_1(q_1, E)|^2$. This relation is similar to an approach for obtaining LDOSs from XAS by Ankudinov *et al* [16]. The non-dipole contribution $\tilde{S}(q_j, \omega)$ can be analysed separately by subtracting the dipole contribution from the dynamic structure factor for other q-values: $\tilde{S}(q_j, \omega) = S(q_j, \omega) - |M_1(q_j, E)|^2 \rho_1(E)$.

3. Results and discussion

3.1. Numerical tests

We start by testing the feasibility of the scheme outlined in the previous section on simulated data. First, we calculate the dynamic structure factor $S(q_i, \omega)$ and matrix elements for the boron K-edge in MgB_2 for several values of momentum transfer. Various choices in the computational scheme affect the accuracy of the results. Since we work with density functional theory (DFT)-type approximations [17], the first choice is the selection of the exchange–correlation potential V_{xc}. We use two choices: the first is a ground state local density approximation V_{xc} proposed by von Barth and Hedin (BH) [18], which does not include quasiparticle effects. In contrast, the second choice, which is appropriate for excited states, is based on work by Hedin and Lundqvist (HL) [19], and replaces V_{xc} by a complex-valued and energy-dependent electron self-energy $\Sigma(E)$. This quantity is based on the local density approximation and the plasmon pole approximation for the electron gas dielectric function. Essentially $\Sigma(E)$ is a dynamically screened exchange–correlation potential, which can account for inelastic losses that are not part of standard DFT. Such inelastic losses give rise to the photoelectron mean free path and hence play an important role in the analysis of XAS and XRS spectra [1, 20–22]. To test the approach we use the BH V_{xc} both in the LDOS calculation and dynamic structure factor calculation. To demonstrate the effect of the quasiparticle corrections, we use the HL choice. Finally, the radius of the cluster used in the multiple scattering calculations was set to 8.5 Å, i.e., a cluster of 266 atoms. It should be noted that when comparing the calculated spectra to experiments the size of the cluster is an important factor in determining the accuracy of the calculation. However, in the method proposed here we are more interested in matrix elements, which are rather insensitive to the cluster size.

The calculations were performed using three momentum transfers with q equal to 1.11, 2.12, and 5.13 a.u. (in this paper, unless otherwise noted, we use atomic units $e = \hbar = m = 1$ so that distances are in Bohr $a_0 = 0.529$ Å). The comparison between the density of states calculated directly from $G_{LL'}$ and that obtained from the calculated $S(q_i, \omega)$ is shown in figure 1. For theoretical data it is clear from this comparison that our scheme for extracting the density of states performs well. The only problematic region is close to the Fermi level (near ≈ -10 eV), where, without the broadening due to the core hole lifetime, the dynamic structure factor would have no spectral weight. We have used terms up to $l = 5$ when expanding the exponential as given in equation (5). However, the contributions from terms higher than $l = 1$ are small (under 5% and mostly dominated by $l = 2$) in the energy and momentum transfer range studied in this work. We solve equation (8) in least squares sense. In practice this means that having $S(\mathbf{q}, \omega)$ for the three momentum transfers specified above we solve the equation only for the dominant terms, i.e. $l = 0$ and $l = 1$. Adding an extra term with $l = 2$ leads to instabilities when this method is applied to experimental data containing statistical errors and uncertainties in the background subtraction.

Figure 2 demonstrates the effect of a more realistic treatment that includes quasiparticle effects for the final state electron by using an HL energy-dependent $\Sigma(E)$ instead of a static V_{xc}. The comparison shows that at low energies the effect of the quasiparticle corrections is mostly

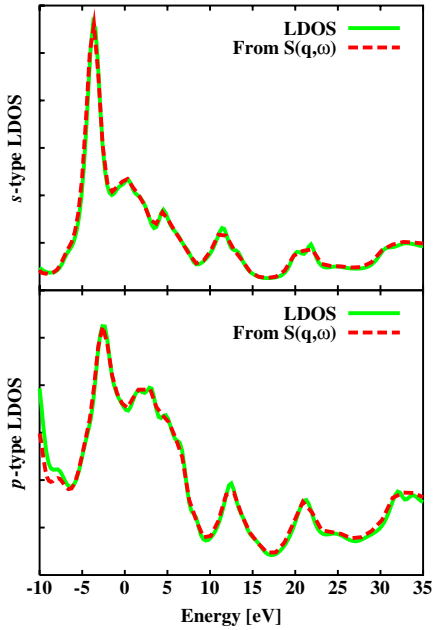

Figure 1. Comparison between the calculated density of empty states and the one obtained through the fitting procedure from the calculated dynamic structure factor. The upper panel shows the comparison for s-type density of states and the lower panel that for p-type density of states. The LDOS is given by the solid line and that obtained from $S(\mathbf{q}, \omega)$ is given by the dashed line.

a broadening of the final LDOS. In certain regions the differences in the exchange correlation potential causes changes in the shape of the final LDOS. For example, for the p-type LDOS the shoulder around 3 eV is more pronounced in the calculation where the BH exchange correlation potential is used. The quasiparticle corrections also affect the position of the peaks due to the energy dependence of Re $\Sigma(E)$. For MgB_2 this effect is strongest around 30 eV above the edge. Additionally the imaginary part of the self-energy Im $\Sigma(E)$ introduces an excitation energy-dependent broadening to the spectra. This represents the excitation energy dependence of the lifetime of the final state electron. The lifetime broadening typically increases slowly in the vicinity of the edge and more rapidly above the plasmon frequency. Finally, in the EXAFS region the broadening due to the finite lifetime of the photoelectron slowly decreases. This is a quite well known effect of the quasiparticle correction but in the following it should be kept in mind that the simple HL approach might not be very accurate in all regions of the spectrum due to the general inadequacy of plasmon pole approximation. Nevertheless, we use the HL approach here because of its low computational cost, although more accurate approaches have recently been developed [22, 23]. Since we know that these quasiparticle effects are important we will use the LDOS calculated with quasiparticle corrections when comparing with experiment.

We have also tested how finite experimental energy resolution affects the proposed method. The experimental energy resolution function can usually be approximated by a Gaussian (or related broadening function) with full width at half maximum ranging from a few tenths of an eV to a few eV. Our scheme relies on the fact that the matrix element is essentially an atomic property, and hence is a relatively smoothly varying function. When we applied our scheme to convoluted spectra, the result was a density of states convoluted with the assumed experimental resolution.

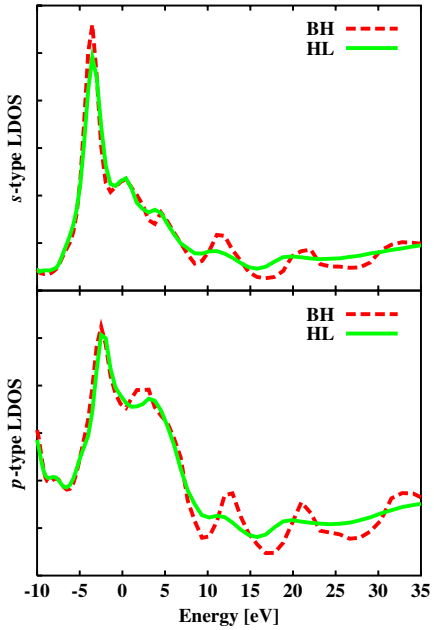

Figure 2. Comparison for the result with (HL $\Sigma(E)$) and without (BH V_{xc}) the quasiparticle corrections. In both cases the results for the density of states were obtained using the proposed fitting scheme. The upper panel shows the comparison for s-type density of states, and the lower panel that for p-type density of states. The result for the BH V_{xc} is given by the dashed line and that for HL is given by the solid line.

3.2. Magnesium diboride experiment

We now apply our method to recently published [12] XRS data for the boron K-edge in MgB_2. The scientific interest in MgB_2 is focused on its superconducting properties and their connection to the electron states near the Fermi level. With our current scheme we can determine the density of states for the core-excited states, and hence separate states with p-type symmetry near the boron atom from those with s-type symmetry. Additionally, we are interested in the density of the p-type states in the boron plane (σ-type) in comparison with density of the p-type states perpendicular to the plane (π-type).

We assume for the MgB_2 boron K-edge that the multiple scattering matrix is diagonal:

$$S(\mathbf{q}, \omega) \approx \sum_l (2l + 1)|M_L(\mathbf{q}, E)|^2 \rho_L(E),$$

i.e. $\rho_{LL'}(E) \approx \delta_{LL'}\rho_L(E)$. The difference compared to the spherically averaged case is that we still have the sensitivity to the direction of $\mathbf{q}$. The comparison between calculated and experimental $S(\mathbf{q}, \omega)$ for the momentum transfers specified earlier is shown in figure 3. The spectra were normalized so that the height of the feature at around 200 eV for momentum transfer in the boron plane ($\mathbf{q} \parallel [100]$) and 209 eV for the momentum transfer perpendicular to the boron plane ($\mathbf{q} \parallel [001]$) were the same for all magnitudes of q. At a qualitative level, the agreement is fairly good and similar to that reported in [12] for the Bethe–Salpeter equation approach [21]. With the momentum transfer in the boron plane the main discrepancy is an overestimation of the peak height around 192 eV. For momentum transfer perpendicular to the boron plane there are small differences for both low and large momentum transfer values. For example, at low momentum transfer the spectral weight of the feature around 195 eV is

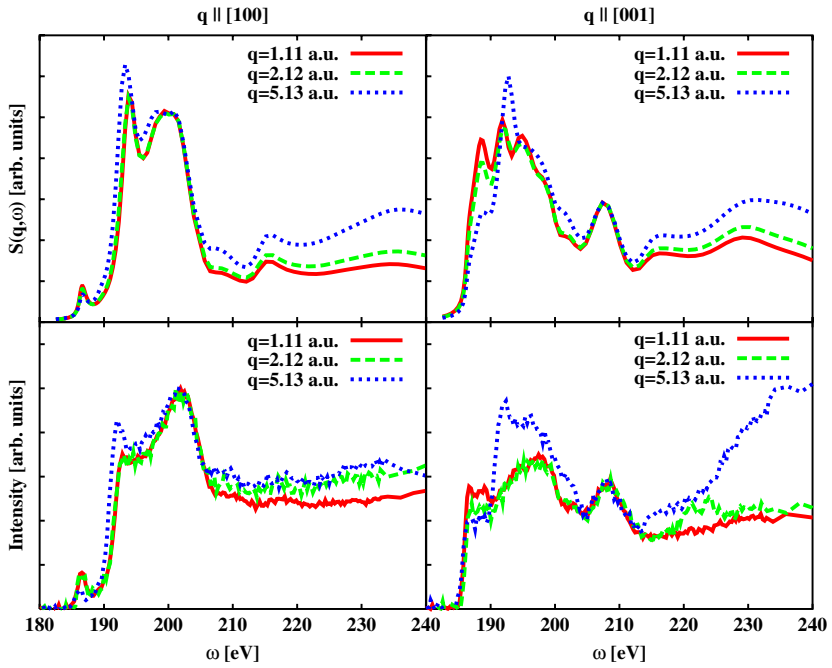

Figure 3. Comparison between experimental (bottom) and calculated (top) XRS spectra for the boron K-edge in MgB_2. The left panel gives the result for the momentum transfers in the boron plane and the right panel the result for momentum transfers perpendicular to it. Magnitudes of the momentum transfers are indicated in the figure.

overestimated when compared to the feature at 209 eV. A similar overestimation of the spectral weight close to the edge has been reported before for light elements for calculations based on multiple scattering approaches [24], as well as for band structure based methods [9, 21]. Also at small momentum transfer there are a number of small peaks in the calculation closer to the absorption edge, whereas the experiment in this energy region is relatively smooth. Overall, the experimental spectra appear smoother than the calculated ones. This is probably due to inadequacies of the simple HL approximation for the final state electron lifetime broadening. Still, the qualitative agreement is such that one can use the calculated matrix elements with good confidence in the fitting process.

Typically, the experimental x-ray Raman spectra are difficult to normalize using the f-sum rule [25], because in most cases only a few tens of eV of the spectrum are measured, and the integration required by the sum rule cannot be done properly. Instead, we use calculated spectra as a reference function for the normalization over a finite energy range. Even with a reference function the small energy window available in the experiment can make the normalization of the data prone to errors. We first subtract from the experimental data the background due to inelastic scattering from the valence and Mg 2s and 2p electrons, as was explained in detail in [12]. We use the calculated atomic background $S_0(q, \omega)$ defined in equation (16) of [14] as a means for normalizing the spectrum. The integration is performed over a small energy window $[E_{\min}, E_{\max}]$ and the experimental dynamic structure factor $S_{\exp}(\mathbf{q}, \omega)$ is scaled so that

$$\int_{E_{\min}}^{E_{\max}} S_{\exp}(\mathbf{q}, \omega) = \int_{E_{\min}}^{E_{\max}} S_0(q, \omega).$$

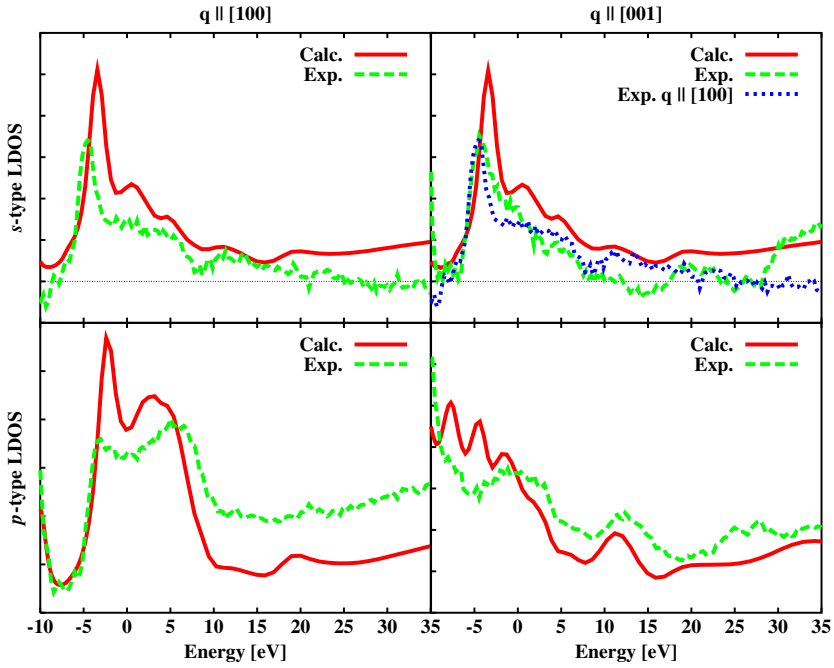

Figure 4. Comparison between the boron site LDOS of MgB_2 determined from experiment (dashed line) and that determined from calculated spectra (solid line). On the left is the LDOS in the boron plane, and on the right is the result for states perpendicular to it. Note that the s-type LDOS in the boron plane is also given on the out-of-plane figure by the dotted line. The horizontal line shows the zero of the y-axis.

Due to the uncertainties in the background subtraction, this method can have a certain sensitivity to the choice of $E_{\min}$ and $E_{\max}$. In general, the background subtraction is most reliable in the region close to the edge as the XRS contribution to dynamic structure factor below the edge has to vanish, and the background function can be typically approximated by a low-order polynomial. On the other hand, $S_0(q, \omega)$ does not have fine structure due to multiple scattering processes. The fine structure should average to zero when integrated to infinitely high excitation energies, so with a finite integration range one is always introducing small errors to the normalization. Alternatively, one could use the calculated $S(\mathbf{q}, \omega)$ as a reference function, but in that case a small deviation in the peak positions could produce even greater error at same values of $E_{\min}$ and $E_{\max}$ than neglecting the fine structure. We have made numerous calculations with different choices of $[E_{\max}, E_{\min}]$ in order to study the sensitivity of the fitting procedure on the energy range used in the normalization. These tests show that choosing too small $E_{\max}$ creates vertical shifts as well as normalization errors. However, the general shape of the final LDOS is rather insensitive to this choice. Overall, it seems important not to be reluctant to use a higher $E_{\max}$ for fear of uncertainties in the background subtraction.

In the following we will concentrate on the directional local density of states at MgB_2 boron sites. Comparison between the calculated LDOS and that derived from experiment using our proposed scheme can be seen in figure 4. As with the dynamic structure factor, the agreement is quite good also for the LDOS[4]. For the p-type LDOS the difference between

[4] The small difference in the energy resolution between the high- and low-momentum transfer spectra reported in [12] has almost no visible effect on the final LDOS.

the σ type and out-of-plane π-type states is clear. For the π-states perpendicular to the boron plane there is a strong contribution from states close to the Fermi energy, whereas σ-states have narrow-band LDOS close to the Fermi energy, followed by a distinct gap. The s-type LDOS is almost zero in a region close to the Fermi energy and shows a distinct peak around -3 eV. The largest differences between the calculated LDOS and that derived from experiment are in the p-type LDOS. The calculated π-LDOS shows more structure in the region from -10 to -2 eV than the LDOS derived from the experiment. Also, the height of the peak structure between -5 and 10 eV for the σ-LDOS is overestimated in the calculation with respect to the broad tail above 10 eV. The difference in these relative heights when compared to experiment could in part be due to uncertainties in the background correction of the experimental data for the energies above 10 eV. This can also be seen in the underestimation of the s-type LDOS which even becomes negative for the $\mathbf{q} \parallel [001]$ case at these energies. The overall agreement is otherwise very good with, for example, the peak between 10 and 15 eV in the π-LDOS nicely reproduced both in height and width.

4. Conclusions

We have studied in detail a recently proposed [14] scheme for extracting the local density of states from momentum transfer-dependent XRS experiments. We carried out a number of numerical tests which confirm that the scheme is stable, and we also studied the effects of quasiparticle corrections on the results. As a practical application the technique was successfully applied to the recently discovered superconductor MgB_2. In particular, we showed that the σ-, π- and s-types of local density of states could be extracted from a recent XRS experiment [12] on the MgB_2 boron K-edge, reaffirming the conclusions presented in the original article. We have further conducted a detailed comparison between the calculated LDOS and the LDOS derived from the experiment using our proposed scheme. Our results for MgB_2 clearly show that the scheme can be applied in XRS to extract the symmetry-resolved LDOS.

Acknowledgments

This work was supported by the Academy of Finland (Contract No 201291/205967/110571), and for JJR by the US Department of Energy (Grant DE-FG03-97ER45623), and was facilitated by the DOE Computational Materials Science Network.

References

[1] Rehr J J and Albers R C 2000 *Rev. Mod. Phys.* **72** 621
[2] Schülke W 1991 *Handbook of Synchrotron Radiation* vol 3, ed G S Brown and D E Moncton (Amsterdam: North-Holland) p 565
[3] Hämäläinen K and Manninen S 2001 *J. Phys.: Condens. Matter* **13** 7539
[4] Mizuno Y and Ohmura Y 1967 *J. Phys. Soc. Japan* **22** 445
[5] Bergmann U, Glatzel P and Cramer S P 2002 *Microchem. J.* **71** 221
[6] Doniach S, Platzman P M and Yue J T 1971 *Phys. Rev.* B **4** 3345
[7] Krisch M H, Sette F, Masciovecchio C and Verbeni R 1997 *Phys. Rev. Lett.* **78** 2843
[8] Soininen J A, Hämäläinen K, Caliebe W A, Kao C-C and Shirley E L 2001 *J. Phys.: Condens. Matter* **13** 8039
[9] Hämäläinen K, Galambosi S, Soininen J A, Shirley E L, Rueff J-P and Shukla A 2002 *Phys. Rev.* B **65** 155111
[10] Sternemann C, Volmer M, Soininen J A, Nagasawa H, Paulus M, Enkisch H, Schmidt G, Tolan M and Schülke W 2003 *Phys. Rev.* B **68** 035111
[11] Sternemann C, Soininen J A, Huotari S, Vankó G, Volmer M, Tse J S and Tolan M 2005 *Phys. Rev.* B **72** 035104
[12] Mattila A, Soininen J A, Galambosi S, Huotari S, Vankó G, Zhigadlo N D, Karpinski J and Hämäläinen K 2005 *Phys. Rev. Lett.* **94** 247003

[13] Mahan G D 1981 *Many-Particle Physics* (New York: Plenum) chapter 8
[14] Soininen J A, Ankudinov A L and Rehr J J 2005 *Phys. Rev.* B **72** 045136
[15] Leapman R D, Rez P and Meyers D F 1980 *J. Chem. Phys.* **72** 1232
[16] Ankudinov A L, Nesvizhskii A I and Rehr J J 2001 *J. Synchrotron Radiat.* **8** 92
[17] Hohenberg P and Kohn W 1964 *Phys. Rev.* **136** B864
Sham L J and Kohn W 1965 *Phys. Rev.* **140** A1133
[18] von Barth U and Hedin L 1972 *J. Phys. C: Solid State Phys.* **5** 1629
[19] Hedin L and Lundqvist B I 1971 *J. Phys. C: Solid State Phys.* **4** 2064
[20] Shirley E L 1998 *Phys. Rev. Lett.* **80** 794
[21] Soininen J A and Shirley E L 2001 *Phys. Rev.* B **64** 165112
[22] Soininen J A, Rehr J J and Shirley E L 2005 *Phys. Scr.* T **115** 243
[23] Rehr J J, Kas J J, Prange M P, Vila F D, Ankudinov A L, Campbell L W and Sorini A B 2006 *Preprint* arXiv:cond-mat/0601242
[24] Ankudinov A L, Nesvizhskii A I and Rehr J J 2003 *Phys. Rev.* B **67** 115120
[25] Nagasawa H, Mourikis S and Schülke W 1997 *J. Phys. Soc. Japan* **66** 3139